JTTEE5 7:505-512

PEER REVIEWED

Numerical Study of an ArH_2 Gas Mixture Flowing Inside and Outside a dc Plasma Torch

P. Eichert, M. Imbert, and C. Coddet

(Submitted 21 October 1997; in revised form 20 April 1998)

The flow of gas mixtures in a dc plasma torch is studied using the CFD PHOENICS (CFD PHOENICS, Berkeley, CA) code. In the model, the cold gas mixture (300 K), initially constituted of 85 vol% Ar and 15 vol% H, is introduced into a power input zone where it takes energy and is ejected in the surrounding atmosphere at constant pressure (10^5 Pa). The flow is assumed to be in chemical equilibrium. Equations of mass, momentum, and energy are discretized using a control-volume method. The turbulent flow is modeled by a k-ε two-equations model for the turbulent kinetic energy and its dissipation rate. Finally, the algebraic coupling equations set is solved by means of the SIMPLEST algorithm, implemented into the CFD code, using a hybrid interpolation scheme. Results concern the effect of the torch power on the ArH_2 flow. The phenomenon is analyzed through the evolution of velocity and temperature inside and outside the torch. From these calculations, the effect of ambient gas entrainment by the jet is emphasized and a comparison of the level of entrained gas is made with experimental data.

Keywords CFD code, control-volume method, dc plasma, modeling, subsonic jet

1. Introduction

In plasma spraying applications, the coating quality depends of course on the characteristics of the plasma jet. Today, numerical modeling is extensively used for the study of particle behavior into the jet, but little work is devoted to the plasma flow itself. Moreover, the jet is usually modeled only from the nozzle exit (Ref 1-4); therefore, except for more recent work (for example, Ref 5) it is necessary to make assumptions about the exit profiles of quantities (i.e., velocity, enthalpy, or temperature, etc).

This work was concerned with the development of a model for a dc plasma torch implementing the CFD PHOENICS (CFD PHOENICS, Berkeley, CA) code (Parabolic, Hyperbolic, or Elliptic Numerical Integration Code Series). The objective was to predict the plasma jet behavior to understand particular phenomena (e.g., cooling of the jet, mixing, etc.), to guide actual experimental works by defining ranges of values for spraying parameters to be optimized and to help in the definition and design of spray torch nozzles. In the first approach, using the solution procedure of the code, it was decided to study the plasma jet behavior (in particular, the velocity and temperature fields inside the torch) versus the torch characteristics (geometry, electric power, etc.). The gas mixture and the surrounding atmosphere conditions were fixed and considered as boundary conditions.

The final objective was to introduce the effect of the carrier gas injection; therefore, a three-dimensional structure was chosen despite the simple geometry actually considered (straight anode similar to a PT F4 APS torch; Sulzer-Metco, Wohlen, Switzerland).

P. Eichert, M. Imbert, and **C. Coddet,** Laboratoire d'Etudes et de Recherches sur les Matériaux et les Propriétés de Surface, Institut Polytechnique de Sévenans, BP 449, 90010 Belfort Cedex, France; contact C. Coddet at e-mail: christian.coddet@utbm.fr.

2. Mathematical Model

The following assumptions were made to simplify the analysis:

- The plasma flow is steady and assumed to be in local thermodynamic equilibrium (LTE).
- The plasma is optically thin, and no radiation phenomena are taken into account.
- The flow is considered to be in chemical equilibrium (the time scale of the chemical kinetics is faster than the time scale of the dynamic flow).
- The gravity force is negligible compared to the kinetic effects.
- The electric discharge is in steady state with a constant power value, and the electric and magnetic forces are neglected.

2.1 Model

The flow is modeled using governing differential equations that have the general form (in the steady state) of:

$$\text{div}\,(\rho \mathbf{V} \Phi) = \text{div}\,(\Gamma_\Phi \,\text{grad}\,\Phi) + S_\Phi \qquad \text{(Eq 1)}$$

Table 1 Independent variables and transfer coefficients

Equation	Φ	Γ_Φ
Mass	1	...
Momentum	u, v, or w	μ
Energy		
Enthalpy	h	$\alpha = k/C_p$
Temperature	T	$\alpha = \mu/Pr$

where Φ is the dependent variable (Table 1), **V** is the velocity vector, and Γ_Φ is the transport coefficient (Table 1). The source term S_Φ (Ref 6) includes the pressure gradient in the momentum equations, and terms accounting for viscous dissipation effects and for pressure in the energy equation (plus the source term corresponding to the energy input). In spite of the complex phenomena occurring in plasmas, the use of species conservation equations was avoided, assuming chemical equilibrium flow, so that the chemical composition depends only on temperature and pressure.

The model has also to account for the turbulent character of the jet. In regard to the transformation of momentum and energy equations of the Eq 1 type by Favre mass-averaged variables, the transfer coefficients become different when taking into account the new turbulent terms (Ref 7). The effective coefficient in momentum equations is the sum of the molecular viscosity, μ, and the turbulent viscosity, μ_t; the term (μ_t/Pr_t) is added to the transport coefficient in the energy equation. The k-ε turbulence model of Harlow-Nakayama (Ref 8, 9) often employed for the modeling of plasma jets was also adopted in this study, even if its predictive ability is not always close to reality (Ref 10-12). The turbulent model introduces two new differential equations of the Eq 1 form for the calculation of the kinetic energy, k, and of its dissipation rate, ε, whose transfer coefficients and source terms are reported in Table 2.

The turbulent viscosity is determined using the expression:

$$\mu_t = C_\mu C_D \rho k^2/\varepsilon \qquad \text{(Eq 2)}$$

where $C_\mu = 0.5478$ and $C_D = 0.1643$ ($C_\mu C_D = 0.09$) (Ref 6). μ_t provides the coupling of the turbulence model for the Navier-Stokes and the energy equations.

A source term was included into the energy equation corresponding to the electric energy input. The arc current, I (A), and voltage, U (V), permit definition of the power applied to the torch. The arc effect, which should necessitate complex modeling (Ref 13-15), is simulated by a total volumic power input expressed as:

$$P_w = UI \qquad \text{(Eq 3)}$$

This energy input is included in the energy equation through a source term corresponding to a total volumic power (W/m^3) applied to a volumic cell (m^3). For calculations, the applied energy is then represented by a total power input per unit volume given to a volume inside the torch.

Thus, the local arc phenomena are not considered in this article. They are replaced by a source term that considers only the thermal effect of the arc on the gas flow, on an average basis. In fact, the energy input zone is much larger than the arc region because of the limitations of numerical calculations when very high gradients occur. The choice of this method corresponds to the desire of developing a simple approach for the inner part of the torch before needing to develop a complete model of the arc itself.

2.2 Computational Domain and Boundary Conditions

The whole system from the injection of the cold gas mixture into the torch to the external development of the plasma jet into the surrounding atmosphere (10^5 Pa) was modeled as a single

Nomenclature

a	algebraic equation coefficient, kg/s
b	linear source term
C_p	specific heat, J/kg · K
d	nozzle diameter, mm
F_m	gas mass flow rate, g/s
F_v	gas volume flow rate, NL/min
h	specific enthalpy, J/kg
I	arc current, A
k	turbulent kinetic energy, m^2/s^2
P	pressure, Pa
P_k	production rate of kinetic energy
P_n	acquired power, W
P_w	total power input, W
Pr	Prandtl number
Pr_t	turbulent Prandtl number
r	radial distance along the y-axis, m
S_Φ	source term of the Φ equation
T	temperature, K
T_{exit}	torch exit temperature, K
T_p	wall temperature, K
T_{room}	room temperature, K
u	velocity component/x-axis, m/s
U	arc voltage, V
v	velocity component/y-axis, m/s
w, W	velocity main component/z-axis, m/s
W_{exit}	torch exit velocity component, m/s
z	axial distance along the z-axis, m
ε	dissipation rate of k
Φ	dependent variable
η	torch efficiency, %
λ	thermal conductivity, W/m · K
μ	dynamic viscosity, kg/m · s
μ_t	turbulent dynamic viscosity, kg/m · s
ρ	density, kg/m^3
Γ_Φ	transport coefficient in the Φ equation

Indicies

i	neighbor cells
k	turbulent kinetic energy
p	pole/node
t	turbulent
ε	dissipation rate of k

Table 2 Transfer coefficients and source terms for the k-ε model (Ref 6)

Variable	Γ_Φ	S_Φ
k	$\mu + \frac{\mu_t}{Pr_{t,k}}$	$\rho(P_k - \varepsilon)$
ε	$\mu + \frac{\mu_t}{Pr_{t,\varepsilon}}$	$\rho \frac{\varepsilon}{k}(C_{\varepsilon 1}P_k - C_{\varepsilon 2}\varepsilon)$
	$Prt,_k = 1$	$Prt,_\varepsilon = 1.3$
	$C_{\varepsilon 1} = 1.44$	$C_{\varepsilon 2} = 1.92$

entity. The plasma is generated by the electric energy injected in a region of the flow and representing the electric arc as indicated above. Figure 1 presents a scheme of the computational domain.

As far as possible, the spray parameters should be treated as conditions for the calculation in order to build a useful code. The identified parameters concerning the actual area of interest are the following.

Firstly, the thermal spray process is considered at atmospheric pressure (APS type). So, at the outer boundary, the pressure is fixed to 10^5 Pa and the temperature to 300 K; gradients of other quantities are considered as null. The entire domain consists of the same fluid.

Secondly, the anode geometry is cylindrical with a diameter of 8 mm and a length of 45 mm. The cathode geometry was not included because it has little effect with a pseudoaxial injection of the gas mixture. The walls of the anode were considered to have a constant temperature equal to $T_p = 650$ K along the energy input zone and $T_p = 300$ K for other zones (i.e., before the energy input zone and outside). A no-slip condition was employed and combined with boundary conditions near walls corresponding to a turbulent log-law of the wall (Ref 16, 17) in order to calculate the velocity component parallel to the wall and k and ε near the wall.

Finally, the initial gas mixture was chosen to consist of 85 vol% Ar and 15 vol% H with a total flow rate $F_v = 90$ NL/min. Of course, the gas composition changes with the energy input along the torch, and then the fluid properties are highly variable.

2.3 Gas Mixture/Plasma Properties

Due to the large temperature variations, one major problem during the study of plasma flows is to take into account realistic plasma properties (i.e., the thermodynamic data and transport coefficients). In the present case, the thermodynamic data are mainly represented by the specific enthalpy and the specific heat while the transport coefficients are the kinematic viscosity and the Prandtl number, which can be determined using the dynamic viscosity, the specific heat, and the thermal conductivity.

Data were taken essentially from the work of Boulos et al. (Ref 18) in which thermodynamic data and transport coefficients of ArH_2 mixtures were computed from the composition of the gas mixture obtained at different temperatures and at constant pressure. The data for the ArH_2 mixture were expressed in polynomial forms depending on the temperature and then, the relationships were programmed within a subroutine of the code. These data permitted determination of the values of the transport coefficients from the local/cell temperatures obtained during the solution procedure (the temperature is calculated using the value of the specific enthalpy, which is the dependent variable of the energy equation). In the entire domain, the plasma properties change from cell to cell with the local temperature in accordance with the chemical equilibrium.

2.4 Discretization Method and Solution Method

The PHOENICS code (Ref 6) solves for a system of conservation equations of "semi-elliptic" type, that is, elliptic partial differential equations. The downstream-to-upstream influence is calculated through the pressure, and the "marching integration" procedure (Ref 19) is used and acts repetitively (e.g., sweeps) on the predominant direction z, solving successively each *YX slab/plane*. A control-volume implicit discretization approach is used in which the domain is subdivided into grid cells (details about this approach can be found in Ref 8, for example). This approach is attractive because it conserves flow quantities locally and globally. A nonstaggered grid technique is used for velocity components.

For each cell, the integration of the differential conservation equations of the general form (Eq 1) over the cell, with suitable interpolation assumptions, leads to a system of nonlinear and coupled algebraic equations of the following form constructed for each grid cell and each variable Φ.

$$a_p \Phi_p = \Sigma a_i \Phi_i + b \qquad \text{(Eq 4)}$$

where the coefficients a_i (kg/s) are functions of Φ variables including convection and diffusion, b being the linear source term, p and i being the pole/node and neighbor cells indices, respectively. The hybrid interpolation scheme, explained by Patankar (Ref 8), is used for the estimation of the Φ and Φ gradients into the cells.

Finally, the solution essentially involves the following dependent variables: Φ, relative pressure (P), velocity components (u, v, w), specific enthalpy (h), turbulent kinetic energy (k), and its dissipation rate (ε). The pressure is obtained indirectly during the solution procedure by the "pressure correction equation" (Ref 8), which is the transformed continuity equation using the corrected expressions of the velocity components during the sweeps/iterations.

The system of equations of the form Eq 4 is solved using the SIMPLEST algorithm (Ref 20) (a modified version of the Semi-Implicit Method for Pressure-Linked Equations algorithm, Ref 21, Fig. 2), which permits solution of the coupling

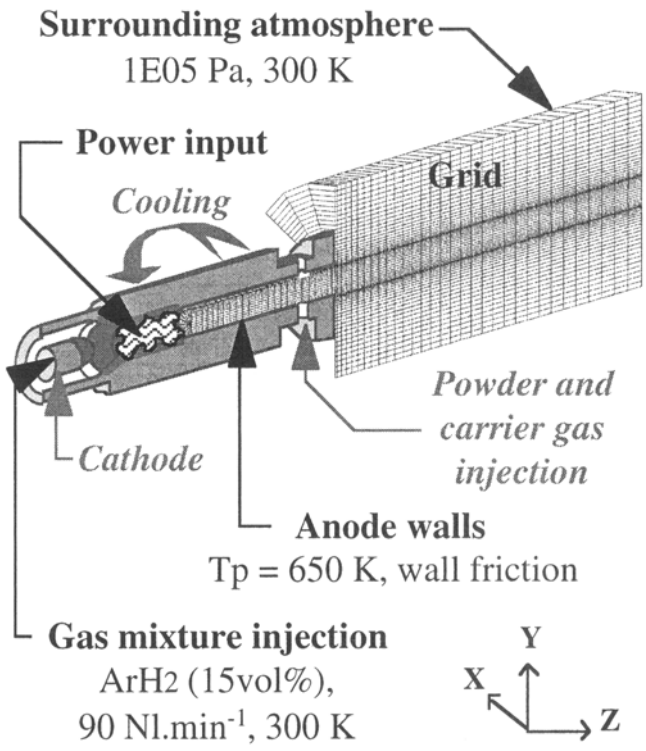

Fig. 1 Computational domain geometry and boundary conditions

between continuity and momentum equations through pressure; in SIMPLEST, the coefficients of Eq 4 contain only the diffusion term while the convection term is added to the source b (Ref 22).

3. Results and Discussions

Results presented here are issued from calculations using the following parameters:

- The anode is cylindrical with a diameter of $d = 8$ mm.
- The total flow rate is $F_v = 90$ NL/min ($F_m = 2.06$ g/s) 85 vol% Ar and 15 vol% H.
- The anode wall temperature is $T_p = 650$ K (except for the walls before the energy input zone and for the external ones for which temperature is fixed to $T_p = 300$ K).

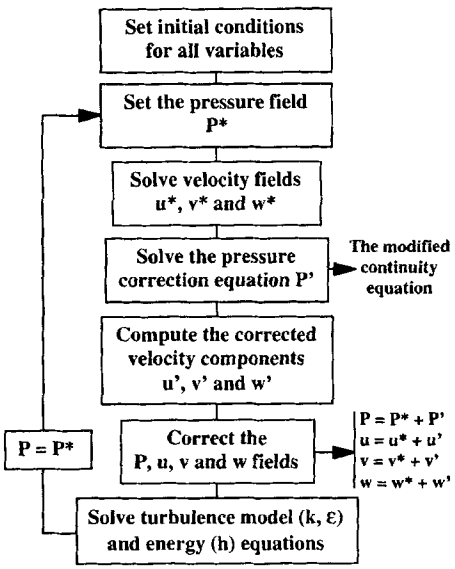

Fig. 2 Functioning principle of the SIMPLE algorithm

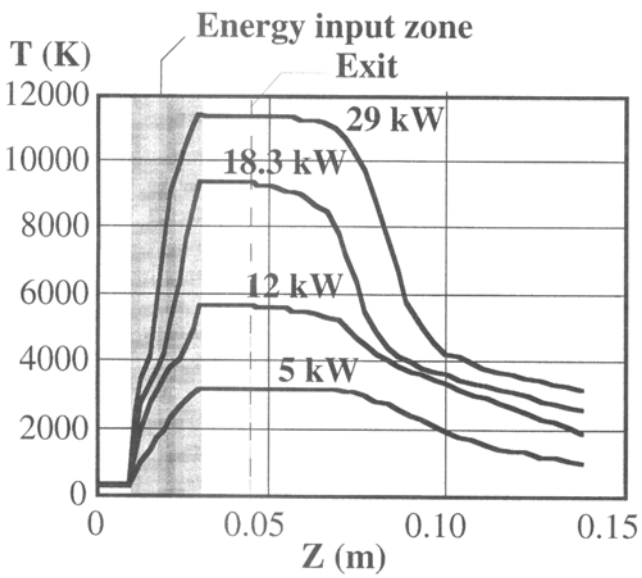

Fig. 3 Axial profiles of temperature (K) inside and outside the torch for different power levels

- Electric power input into the gas flow are, respectively: $P_w = 5$, 12, 18.3, and 29 kW.
- The ambient atmosphere is composed by the studied fluid at 300 K and its pressure is 10^5 Pa.

3.1 Axial Profiles Inside and Outside the Torch

Due to the important gradients that are created in the system and that are not easily accommodated for the numerical scheme, the method applied was the following: the given energy was applied to a 20 mm length zone to expand the discontinuity zone and was progressively increased during the calculation procedure. The corresponding relaxation coefficient values had to be tested and optimized, but no important numerical problem was observed even if the curves do not evolve regularly into this zone.

Figures 3 and 4 display axial profiles of the centerline values of temperature and velocity from the injection point of the cold gas mixture to the jet expansion zone outside the torch exit. Previous calculations (Ref 23) have shown that the Mach number never exceeds 0.65 so that observations can be made relative to free subsonic jets. The increase of all values of temperature and velocity can be observed together with curve inflections in the zone of energy input. In fact, the energy input in the flow generates chemical phenomena such as dissociation and ionization that modify the composition of the gas mixture (see for example Fig. 5) according to the temperature increase. Therefore, the enthalpy (see for example Fig. 6), the thermodynamic data, and the transport coefficients that are dependent on the composition of the gas mixture do not evolve linearly with the temperature.

Concerning the studied ArH_2 mixture, no chemical reactions exist between the species, but dissociation and ionization phenomena occur. For the specific heat (Fig. 7a), the first peak (near 3500 K) corresponds to the dissociation of hydrogen molecules and the second one (near 14,000 K) corresponds to the ionization of the argon and hydrogen atoms. Due to the important variation of the gas composition, the transport coefficients show

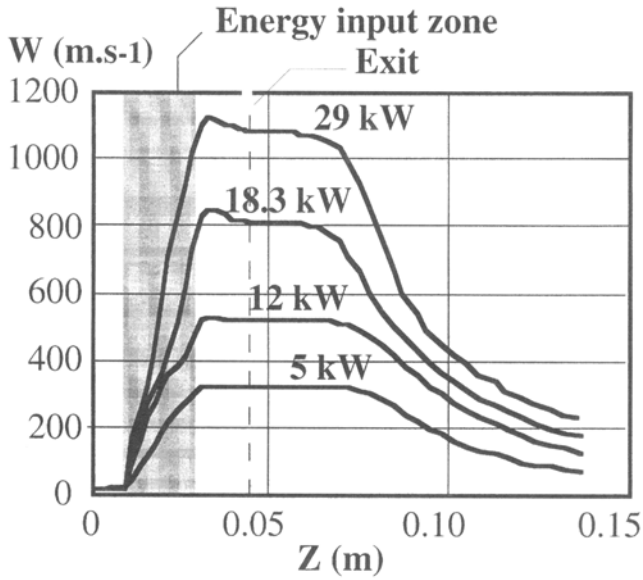

Fig. 4 Axial profiles of velocity (m/s) inside and outside the torch for different power levels

variable evolutions (Fig. 7b and 7c) as well as the resulting Prandtl number (Fig. 7d). The most important variations appear around 3500 K with temperature corresponding to the first peak of the specific heat curve (Fig. 7a). Looking at Fig. 3 for the axial temperature evolution, it is also possible to observe that the large curve inflections in the energy input zone and in the surrounding atmosphere correspond to temperatures between 3000 and 5000 K. The observed nonlinear evolutions of the temperature and velocity profiles are then directly related to the nonlinear evolutions of the transport properties in the range of temperatures concerned by high variations of the gas composition.

At the end of the energy input zone (Fig. 3 and 4), quantities have reached their maximum value and a plateau of near-constant value takes place until a few centimeters after the torch exit (between 1.5 and 3 cm). This plateau corresponds to the thermal and dynamic cores for the temperature and the velocity, respectively, with lengths that seem to be as much dependent on the transport phenomena as on the applied power value (Ref 23). Within the present range of power values, the evolution of the maximum value of temperature and velocity is an increasing function, but it cannot be fitted by a simple law.

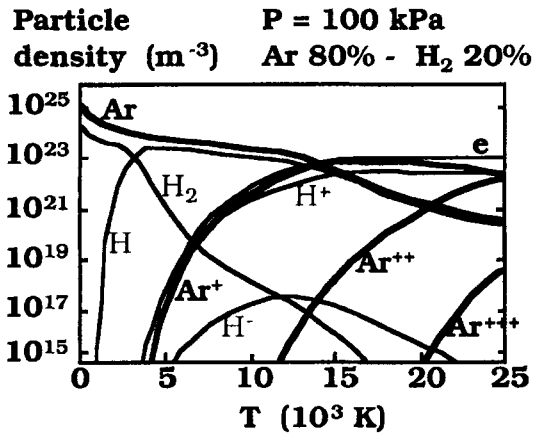

Fig. 5 Particle (species) density versus the temperature of an ArH_2 mixture (Ref 18)

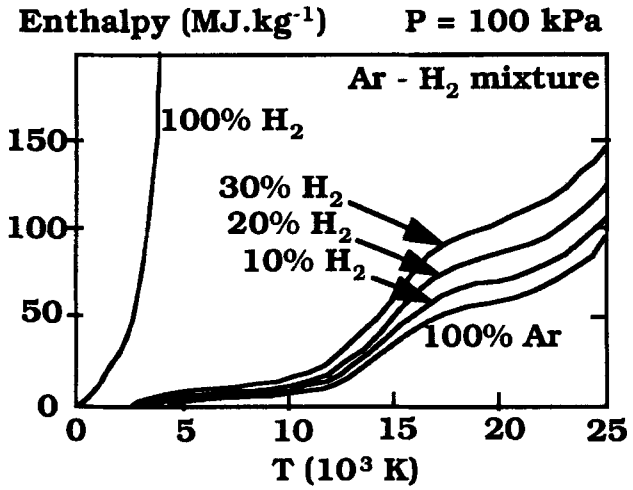

Fig. 6 Enthalpy evolution versus the temperature of ArH_2 mixtures (Ref 18)

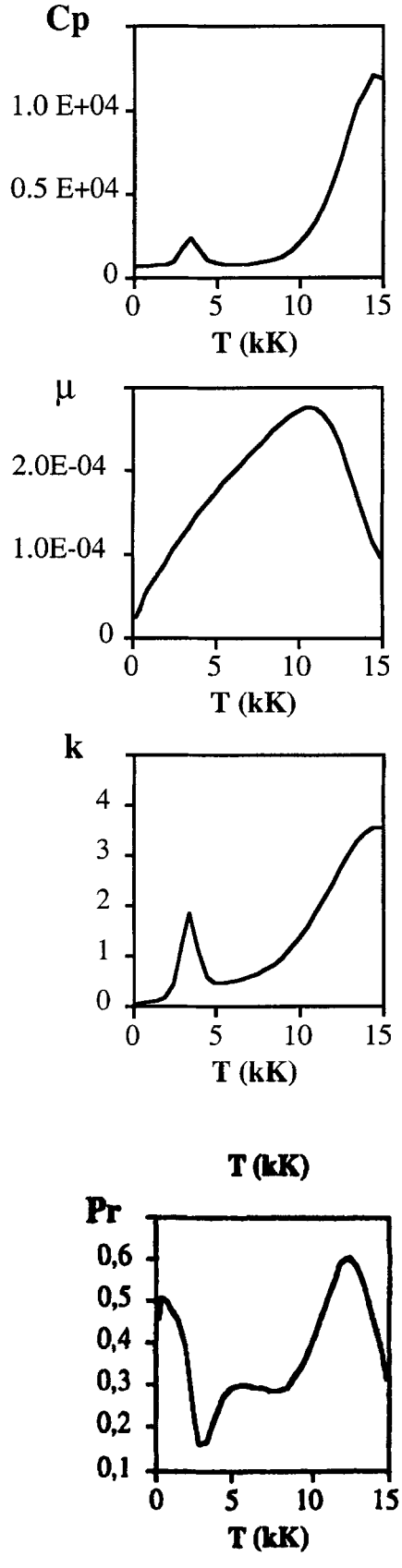

Fig. 7 Evolution versus the temperature of (a) the specific heat, (b) the dynamic viscosity, (c) the thermal conductivity, and (d) the Prandtl number, for the 85 vol% Ar and 15 vol% H mixture

In the surrounding atmosphere (Fig. 3 and 4), especially in the region between the core and the zone of fully developed jet, gradients are more important for the higher energy input values (i.e., 18.3 and 29 kW), which correspond to important dissipative exchanges between the jet and the surrounding gas. These pronounced decreasing evolutions appear between 12 and 18.3 kW, where the slope of the curves become different.

Table 3 Torch exit centerline temperature (K) and main component velocity (m/s) values for different power levels (kW)

	P_w, kW			
	5	12	18.3	29
T_{exit}, K	3245	5674	9304	11,370
W_{exit}, m/s	333	525	809	1,075

Table 4 Losses and efficiency calculations for the different power levels

P_w, kW	P_n, kW	Losses, kW	η, %
5	3.753	1.247	75
12	7.926	4.074	66
18.3	11.826	6.474	65
29	17.732	11.268	61

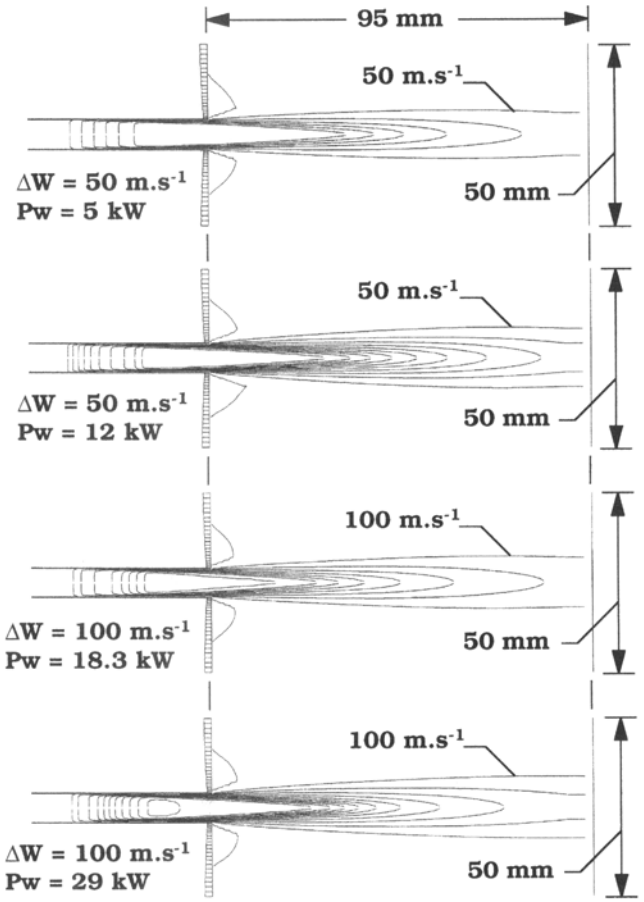

Fig. 8 Velocity isocontours (m/s) for different power levels (kW)

3.2 Velocity and Temperature Isocontours

Figures 8 and 9 display, respectively, the velocity and temperature isocontours for the different power levels. A progressive increase of velocity and temperature inside the energy input zone and the evolution of the jet expansion depending on the power input are observed. Table 3 presents the centerline values of temperature and velocity at the torch exit. The thermal and dynamic cores from the torch exit up to a few centimeters can be visualized observing the isocontours of higher values.

Table 4 shows the calculation of the energy losses inside the torch. The losses were calculated from the energy balance. The difference between the energy content of the gas at the torch exit and its value at the entry gives the amount of energy acquired by the fluid. The losses correspond also to the difference between the amount of applied energy (P_w) and that acquired by the fluid at the exit of the torch. Finally, the torch efficiency is the ratio of the net power input into the gas, P_n, to the applied power value (P_w). It can be observed that the efficiency obtained by calculation ($\eta = 61\%$) for $P_w = 29$ kW is close to the experimentally obtained value for similar parameters by Vardelle ($\eta = 63\%$, Ref 24).

3.3 Ambient Gas Entrainment

The entrainment of the ambient fluid is a well-known phenomenon (Ref 25, 26), but its study has been essentially experi-

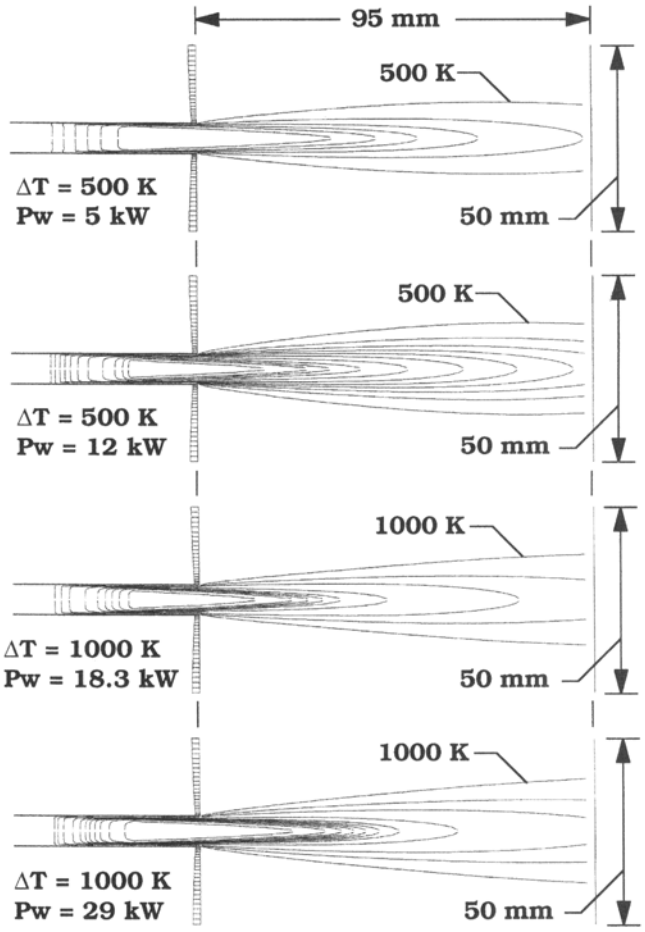

Fig. 9 Temperature isocontours (K) for different power levels (kW)

mental up to now. Figure 10 displays the coefficient of entrainment of the ambient fluid (a) and the plasma gas fraction in the total flow rate (b) versus the axial distance (z).

In the literature (Ref 11), the entrainment along the jet axis (z) and through cross sections of the jet is defined as:

$$\text{Entrainment}(z) = \left(\frac{\text{Total flow rate of gases on } z \text{ location}}{\text{Initial gas flow rate on } z = 0}\right) - 1 \quad \text{(Eq 5)}$$

This relationship was used for the present calculations in a cross section of diameter corresponding to 6.25 times the nozzle diameter (i.e., 50 mm). At $z = 20$ mm, the plasma jet has entrained 1.8 to 2.5 times its flow rate of external fluid. At $z = 80$ mm (e.g., 10 times the nozzle diameter), the entrainment reaches 8 to 11 times the initial flow rate in the concerned range of power values. The entrainment seems to follow a relatively linear evolution with power, except for $P_w = 5$ kW where the evolution of this quantity is modified after $z = 50$ mm, probably because of a large density increase due to the high cooling of the jet.

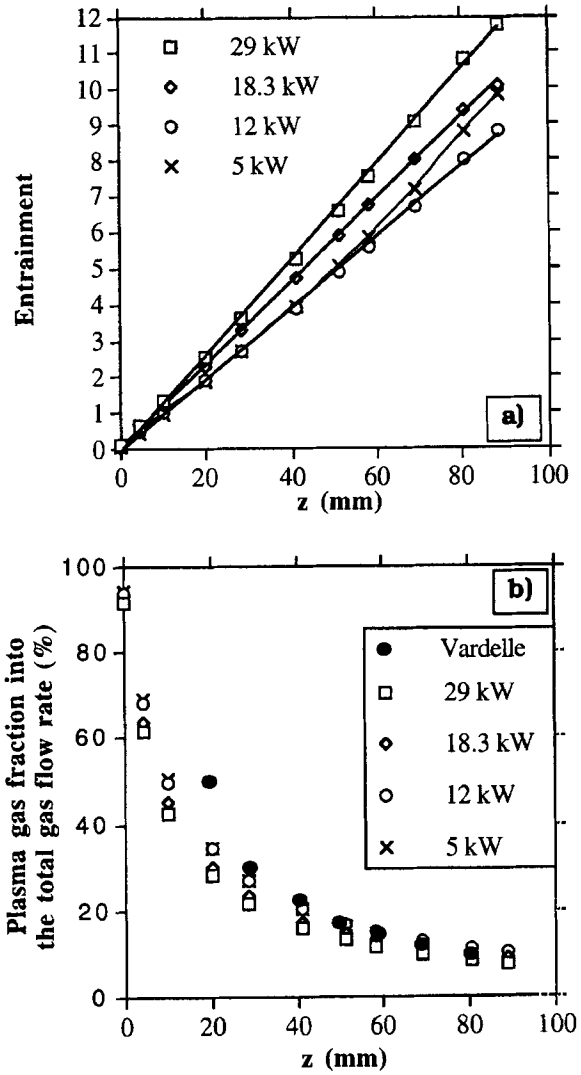

Fig. 10 Ambient gas into the plume. (a) Entrainment. (b) Plasma gas fraction compared to the total flow rate and comparison with experimental data for 29 kW (Ref 24).

On the other side, the plasma gas fraction (%) corresponds to the ratio of the ejected plasma flow rate to the total flow rate through cross sections of the jet. For an ArH_2 (17.6 vol%) jet submitted to an electric power equal to $P_w = 29$ kW, Vardelle (Ref 24) has calculated that the plasma gas fraction represents 50% at $z = 20$ mm of the torch exit, around 20% at $z = 40$ mm, and only around 10% at $z = 80$ mm. As can be observed in Fig. 10(b), similar results are observed in the authors' calculations. In all cases, after $z = 80$ mm, the plasma gas fraction corresponds to less than 10% of the total quantity of the flowing gases.

4. Conclusion

The present numerical work focused on the study of the effect of the electric power input on the flow of an ArH_2 plasma. The studied domain includes the inside of the torch where gases acquire energy (i.e., the progressive increase of temperature and velocity) and the external atmosphere where the plasma jet expands and entrains the ambient fluid. The electric arc modeling was not considered, and the electric energy was simplified as a volumic power input inside the torch. This scheme allows temperature and velocity profiles to be obtained at the torch exit as a result of basic phenomena occurring inside the torch, and consequently no assumptions were necessary for profile shapes at the torch exit. General characteristics of the thermal free jets were observed, that is, dynamic and thermal cores and important drop of quantities along the axial distance. Thus, the model represents the temperature and velocity evolutions in a satisfactory manner. Further developments will be necessary for its application to different gases mixtures and also to take into account the powder carrier gas injection.

References

1. A.H. Dilawari and J. Szekely, Fluid Flow and Heat Transfer in Plasma Reactors—I. Calculation of Velocities, Temperature Profiles, and Mixing, *Int. J. Heat Mass Transfer*, Vol 30 (No. 11), 1987, p 2357-2372
2. A.H. Dilawari, J. Szekely, J.F. Coudert, and P. Fauchais, Fluid Flow and Heat Transfer in Plasma Reactors—II. A Critical Comparison of Experimentally Measured and Theoretically Predicted Temperature Profiles in Plasma Jets in the Absence and Presence of Side-Stream Injection, *Int. J. Heat Mass Transfer*, Vol 32 (No. 1), 1989, p 35-46
3. A.H. Dilawari, J. Szekely, J. Batdorf, R. Detering, and C.B. Shaw, The Temperature Profiles in an Argon Plasma Issuing into an Argon Atmosphere: A Comparison of Measurements and Predictions, *Plasma Chem. Plasma Process.*, Vol 10 (No. 2), 1990, p 321-337
4. A.H. Dilawari, J. Szekely, and R. Wesrhoff, A Comparison of Experimental Measurements and Theoretical Predictions Regarding the Behavior of a Turbulent Argon Plasma Jet Discharging into Air, *Plasma Chem. Plasma Process.*, Vol 10 (No. 4), 1990, p 501-513
5. A.B. Murphy and P. Kovitya, Mathematical Model and Laser-Scattering Temperature Measurements of a Direct-Current Plasma Torch Discharging into Air, *J. Appl. Phys.*, Vol 73 (No. 10), May 1993, p 4759-4769
6. The Phoenics Reference Manual, CHAM/TR200, CHAM, London, United Kingdom

7. D.A. Anderson, J.C. Tannehill, and R.H. Pletcher, *Computational Fluid Mechanics and Heat Transfer,* Hemisphere Publishing, 1984, 599 pages
8. S.V. Patankar, *Numerical Heat Transfer and Fluid Flow,* Series in Computational Methods in Mechanics and Thermal Sciences, W.J. Minkowycz and E.M. Sparrow, Ed., Hemisphere Publishing, 1980, 197 pages
9. W. Rodi, Turbulence Models and Their Applications, Collection de la direction des études et recherches d'EDF, Vol 2, Eyrolles, Paris, France, 1984, 103 pages (in French)
10. P.C. Huang, E. Pfender, and J. Heberlein, New Modeling Approach for Calculating Particle Trajectories in a Turbulent Plasma Spray Jet, *Thermal Spraying—Current Status and Future Trends,* A. Ohmori, Ed., High Temperature Society of Japan, Vol 1, 1995, p 1159-1163
11. P. Proulx, "Mathematical Modeling of Plasma-Particles Flows," thesis, University of Sherbrooke, 1987, 256 pages (in French)
12. M.M. Jankovic, D.Z. Milojevic, and P.Lj. Stefanovic, Mathematical Model for Calculation of Flow Parameters of Thermal Plasma Jet, *Colloque de Physique C5,* Tome 51, Suppl. No. 18, 1990, p 229-236
13. V.S. Engel'sht, The Theory of the Electric Arc Column, *Thermal Plasma and New Materials Technology,* O.P. Solonenko & M.F. Zhukhov, Vol 1, Cambridge Interscience, 1994, p 44-67
14. A.Zh. Zhainakov, Mathematical Modelling of Electric Arc Plasma Flows, *Thermal Plasma and New Materials Technology,* O.P. Solonenko & M.F. Zhukov, Ed., Cambridge Interscience, Vol 1, 1994, p 121-140
15. I.G. Panevin, Near-Electrode Processes, *Thermal Plasma and New Materials Technology,* Solonenko & Zhukhov, Ed., Cambridge Interscience, Vol 1, 1994, p 204-228
16. B.E. Launder and D.B. Spalding, The Numerical Computation of Turbulent Flows, *Computer Method in Applied Mechanics and Engineering,* North-Holland Publishing, Vol 3, 1974, p 269-289
17. M. Nallasamy, Turbulence Models and Their Applications to the Prediction of Internal Flows: A Review, *Comput. Fluids,* Vol 15 (No. 2), 1987, p 151-194
18. M.I. Boulos, P. Fauchais, and E. Pfender, *Thermal Plasmas: Fundamentals and Applications,* Vol 1, Plenum Press, 1994, 452 pages
19. D.B. Spalding, *GENMIX—A General Computer Program for Two-Dimensional Parabolic Phenomena,* Pergamon Press, 1977, 380 pages
20. D.B. Spalding, *Mathematical Modelling of Fluid Mechanics Heat Transfer and Mass Transfer Processes,* Report HTS/80/1, Imperial College CFDU, United Kingdom, 1980
21. S.V. Patankar and D.B. Spalding, A Calculation Procedure for Heat, Mass, and Momentum Transfer in Three-Dimensional Parabolic Flows, *Int. J. Heat Mass Transfer,* Vol 15, 1972, p 1787
22. D.B. Spalding, "Four Lectures on the PHOENICS Computer Code," CFD/82/5, CFD Unit, Imperial College of Science and Technology, London, Nov 1982, 114 pages
23. P. Eichert, "Study of the Gaseous Flow Inside and Outside a dc Plasma Spray Torch," thesis, University of Franche-Comté, 1996, 239 pages (in French)
24. A. Vardelle, "Numerical Study of Momentum, Mass, and Heat Transfers between a DC Arc Plasma and Solid Particles," thesis, University of Limoges, 1987 (in French)
25. E. Pfender, W.L.T. Chen, and R. Spores, A New Look of the Thermal and Gas Dynamic Characteristics of a Plasma Jet, *Thermal Spray Research and Applications,* T.F. Bernecki, Ed., ASM International, 1990, p 1-10
26. E. Pfender, J. Fincke, and R. Spores, Entrainment of Cold Gas into Thermal Plasma Jets, *Plasma Chem. Plasma Process.,* Vol 11 (No. 4), 1991, p 529-543